UCRL-JC-127961
Preprint

The Effects of Confinement and Temperature on the Shock Sensitivity of Solid Explosives

J. W. Forbes
C. M. Tarver
P. A. Urtiew
F. Garcia

This paper was prepared for submittal to
Eleventh International Detonation (1998) Symposium
Snowmass, CO
Aug. 31- Sept. 4, 1998

August 17, 1998

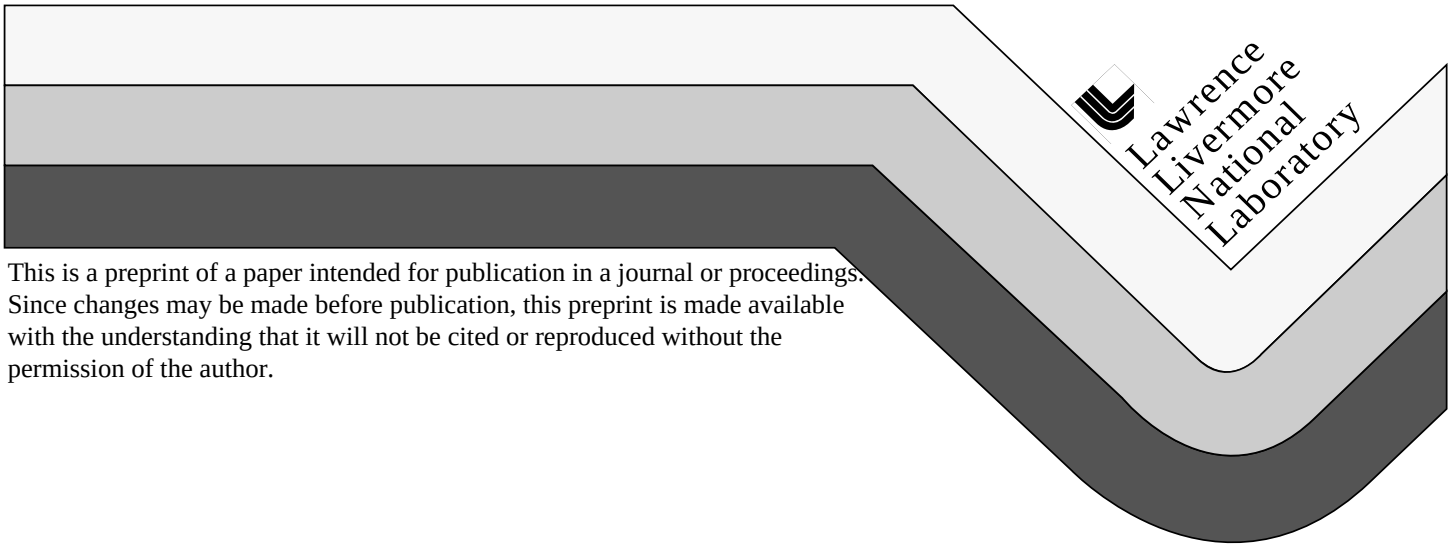

THE EFFECTS OF CONFINEMENT AND TEMPERATURE ON THE SHOCK SENSITIVITY OF SOLID EXPLOSIVES

J. W. Forbes, C. M. Tarver, P. A. Urtiew, and F. Garcia
Energetic Materials Center, L-282
Lawrence Livermore National Laboratory
Livermore, CA 94551

The effects of heavy steel confinement on the shock sensitivity of pressed solid high explosives heated to temperatures close to thermal explosion conditions were quantitatively measured. Cylindrical flyer plates accelerated by a 101 mm diameter gas gun impacted preheated explosive charges containing multiple embedded manganin pressure gauges. The high explosive compositions tested were LX-04-01 (85 wt.% HMX and 15 wt.% Viton A) heated to 170°C and LX-17 (92.5 wt.% TATB and 7.5 wt.% Kel-F) heated to 250°C. Ignition and Growth reactive flow models for heated, heavily confined LX-04-01 and LX-17 were formulated based on the measured pressure histories. LX-17 at 250°C is considerably less shock sensitive when confined by steel than when confined by aluminum or unconfined. LX-04-01 at 170°C is only slightly less shock sensitive when confined by steel than when it is unconfined. The confinement effect is smaller in LX-04-01, because HMX particle growth is much less than that of TATB.

INTRODUCTION

With safety issues playing a dominant role in present-day energetic materials technology, concern is increasing about the relative safety of solid high explosives exposed to extreme environmental conditions. Hazard scenarios can involve multiple stimuli, such as heating to temperatures close to thermal explosion conditions followed by fragment impact, producing a strong shock wave in the hot explosive. High energy materials based on octahydro-1,3,5,7-tetranitro-1,3,5,7-tetrazocine (HMX) and triaminotrinitrobenzene (TATB) are studied in this paper.

Previous research[1-7] using unconfined and weakly confined charges of LX-04-01 (85 wt.% HMX and 15 wt.% Viton A) and LX-17 (92.5 wt.% TATB and 7.5 wt.% Kel-F) showed that the shock sensitivity of the heated charges was significantly greater than that of ambient charges. This increase in shock sensitivity was primarily due to two effects: the increase in the number and size of reacting hot spots formed by shock compression of the thermally expanded charges and the increase in hot spot growth rate into the surrounding preheated explosive particles. In the case of 250°C LX-17, weak confinement by thin aluminum cylinders helped mitigate the initial temperature shock sensitization effect by reducing thermal expansion during the heating process.[5] Thick steel cylinders were employed in this paper to simulate the maximum degree of confinement solid explosives would encounter in practical applications. The steel confinement experiments resulted in decreased shock sensitivity in both LX-04-01 and LX-17. The effect of the steel confinement was greater for LX-17, because the TATB molecule exhibits greater and more asymmetric thermal expansion than HMX. To quantify these effects and to allow shock initiation predictions to be made for scenarios that can not be tested directly, Ignition and Growth reactive flow models for heated, heavily confined LX-04-01 and LX-17 were formulated based on the measured pressure histories and run distances to detonation.

EXPERIMENTAL GEOMETRY

The configuration for the 304 Stainless steel confined shots on heated LX-04-01 and LX-17 is given in Figure 1. The six manganin gauges were

at various depths in the charges for recording the pressure histories. The front steel plate was 9 mm thick and was fastened to the rear steel plate with

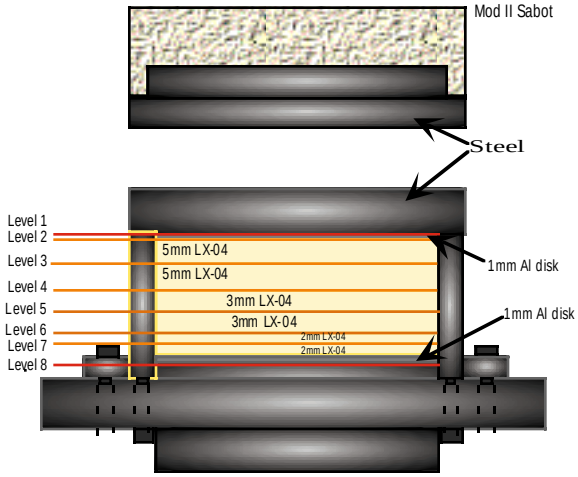

FIGURE 1. GEOMETRY OF THE HEATED AND 304 STAINLESS STEEL CONFINED MANGANIN GAUGE EXPERIMENTS

several steel bolts. Each disc of explosive was radially contained by a close fitting steel ring. The gauge packages contained both thermocouples and manganin pressure gauges between two discs of 0.13 mm thick Teflon armor. The leads for the gauges and thermocouples were brought out the sides between the steel rings which were radially confining the explosive. A 1 mm thick aluminum plate was placed between the front steel plate and the explosive to distribute the heat better than the steel plate would alone. The flat ribbon heater was placed between the steel plate and the aluminum plate. The same heater configuration was placed at the back of the target assembly. PZT pins were placed flush with the face of the target to measure tilt and also nominally 15 mm in front of target face to measure projectile velocity. Flash x-rays are also used to give a second measure of projectile velocity. The ambient shots were done in a similar configuration except for the absence of confinement. The shock loading was produced by a symmetrical impact of a Teflon flyer on a Teflon buffer backed by LX-04-01 discs.

IGNITION AND GROWTH MODELING

The Ignition and Growth reactive flow of shock initiation and detonation of solid explosives has been incorporated into several hydrodynamic computer codes and used to solve many explosive and propellant safety and performance problems.[1-7] The model uses two Jones-Wilkins-Lee (JWL) equations of state, one for the unreacted explosive and another one for its reaction products, in the temperature dependent form:

$$p = A\, e^{-R_1 V} + B\, e^{-R_2 V} + \omega C_V T/V \qquad (1)$$

where p is pressure in Megabars, V is the relative volume, T is temperature, ω is the Gruneisen coefficient, C_V is the average heat capacity, and A, B, R_1, and R_2 are constants. The reaction rate law for the conversion of explosive to products is:

$$dF/dt = I(1-F)^b(\rho/\rho_o - 1 - a)^x + G_1(1-F)^c F^d p^y \qquad (0<F<F_{igmax}) \quad (0<F<F_{G1max})$$

$$+ G_2(1-F)^e F^g p^z \qquad (F_{G2min}<F<1) \qquad (2)$$

where F is the fraction reacted, t is time, ρ is the current density, ρ_o is the initial density, p is pressure in Mbars, and I, G_1, G_2, a, b, c, d, e, g, x, y, and z are constants. As explained more fully in previous papers,[1-7] this three term rate law models the three stages of reaction generally observed in shock initiation of heterogeneous solid explosives. The first term represents the ignition of the explosive as it is compressed by a shock wave creating heated areas (hot spots) as the voids in the material collapse. Generally, the amount of explosive ignited by a strong shock wave is approximately equal to the original void volume.[1] The second term in Eq. (2) represents the growth of reaction from the hot spots into the remaining solid. During shock initiation, this term models the relatively slow spreading of reaction in a deflagration-type process of inward and/or outward grain burning. The exponents on the (1 - F) factors in the first two terms of Eq. (2) are generally set equal to 2/3 to represent the surface to volume ratio for spherical particles. The third term in Eq. (2) describes the rapid transition to detonation observed when the growing hot spots begin to coalesce and transfer large amounts of heat to the

remaining unreacted explosive particles causing them to react very rapidly. In this paper, Ignition and Growth model parameters are developed for 250°C LX-17 and 170°C LX-04-01 heavily confined by steel plates.

COMPARISONS OF EXPERIMENTS AND CALCULATIONS

In this section, the experimental and calculational results are compared for the shots listed in Table 1.

TABLE 1. SUMMARY OF THE STEEL CONFINED 170°C LX-04-01 AND 250°C LX-17 SHOTS

Explosive Charge	Flyer Velocity (km/s)
LX-04-01	0.535
LX-04-01	0.642
LX-04-01	0.725
LX-04-01	0.801
LX-04-01	0.828
LX-17	0.988
LX-17	1.11
LX-17	1.16
LX-17	1.21

The Ignition and Growth model parameters for LX-17 and LX-04-01 are listed in Table 2, and the equation of state parameters for the inert materials are listed in Table 3. Figure 2 shows the manganin gauge records and the corresponding Ignition and Growth calculations for the lowest shock pressure LX-04-01 experiment, which had an impact velocity of 0.535 km/s.

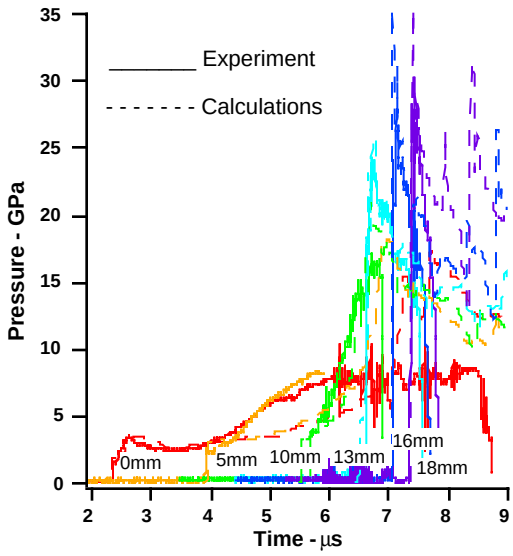

FIGURE 2. PRESSURE HISTORIES FOR STEEL CONFINED 170°C LX-04-01 IMPACTED BY A STEEL FLYER AT 0.535 KM/S

The calculated growth of reaction at the 0 mm and 5 mm gauges is slightly slower than the measurements. However, shock front acceleration, increases in shock front pressure, the growth of reaction at the 10 mm and 13 mm gauges, and detonation traces at 16 mm and 18 mm are all accurately calculated. Figure 3 shows the records for the 0.642 km/s flyer velocity impact on 170°C LX-04-01. The first three gauges were noisy, and this was found to be due leaving the heaters on when the gas gun was fired. In the other shots, the heaters were turned off just before firing the gun, and the resulting gauge records were much less noisy. As in Fig. 2, the early growth of reaction at the 0 mm and 5 mm gauge positions is slightly slow, but the transition to detonation just before the 10 mm deep gauge is correctly predicted. Figure 4 compares the experimental and calculated records for the 0.725 km/s steel impact on 170°C LX-04-01. In this experiment, the gauges were placed near the impact surface to obtain more records at short distances into the explosive. The calculations are in good agreement with the gauge records, and the transition to detonation occurs between the 4 mm deep gauge and the 7 mm deep gauge. The calculations for the two higher velocity 170°C LX-04-01 shots in Table 1, 0.801 km/s and 0.828 km/s, are also in good

agreement, and the transitions to detonation both occur less than 4 mm into the LX-04-01. Thus, the Ignition and Growth model yields good agreement with the five embedded gauge experiments on steel confined 170°C LX-04-01.

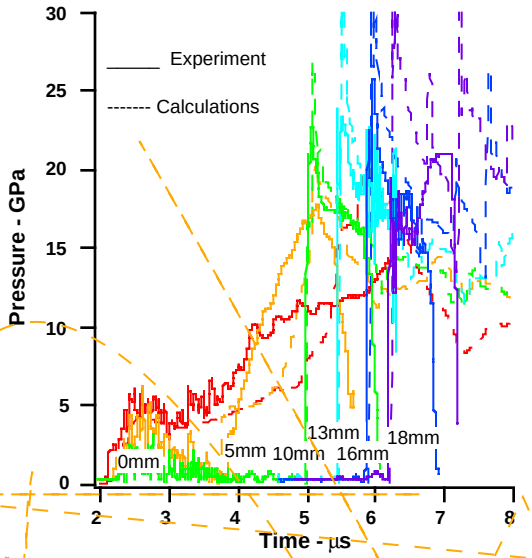

FIGURE 3. PRESSURE HISTORIES FOR STEEL CONFINED 170°C LX-04-01 IMPACTED BY A STEEL FLYER AT 0.642 KM/S

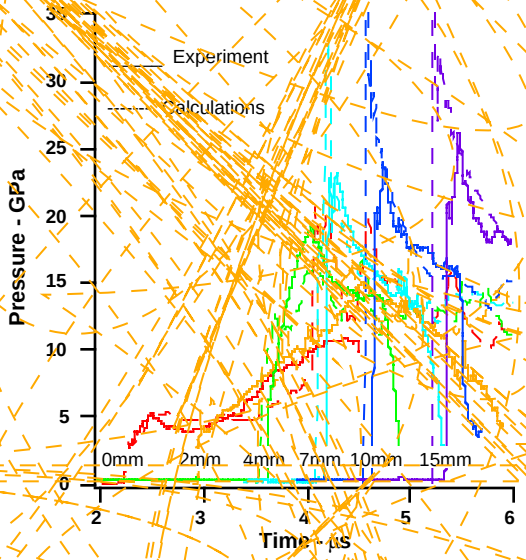

FIGURE 4. PRESSURE HISTORIES FOR STEEL CONFINED 170°C LX-04-01 IMPACTED BY A STEEL FLYER AT 0.725 KM/S

To provide additional data on ambient temperature unconfined LX-04-01, two embedded gauge experiments were fired using Teflon flyer plates. Figure 5 shows the gauge records and Ignition and Growth calculations for ambient temperature LX-04-01 impacted by a Teflon flyer at 1.118 km/s. Figure 6 contains similar curves for ambient temperature LX-04-01 impacted by another Teflon flyer at 1.279 km/s. These two experiments and the ambient LX-04-01 experiment previously reported by Urtiew et al.[7] were modeled with the parameters listed in Table 2 for 170°C LX-04-01 except that the density, temperature, shear modulus, and B value under ambient conditions were used. The growth coefficient G_1 was set equal to 90 Mbar^{-2} μs^{-1}. The previously reported ambient temperature LX-04-01 calculations[7] used a growth coefficient G_1 = 100 Mbar^{-2} μs^{-1} with different, less accurate unreacted and product equations of state.

Figure 7 shows the run distance to detonation versus input shock pressure "Pop Plot" results for LX-04-01 at ambient temperature, 170°C unconfined, and 170°C heavily confined by steel.

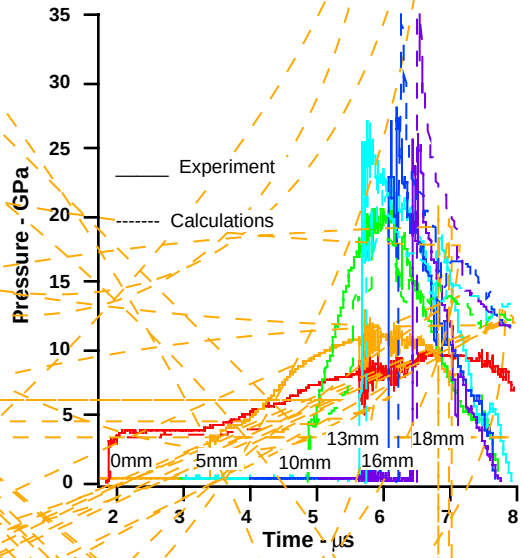

FIGURE 5. PRESSURE HISTORIES FOR UNCONFINED 25°C LX-04-01 IMPACTED BY A TEFLON FLYER AT 1.118 KM/S

The "Pop Plot" shows very little difference between the unconfined 170°C LX-04-01 and the steel confined 170°C LX-04-01. However, the gauge records and the Ignition and Growth parameters do show that the confined 170°C LX-04 is slightly less

parameters listed in Table 2, a growth coefficient G_1 of 190 $Mbar^{-2}\mu s^{-1}$ was required. Urtiew et al.[7] reported a growth coefficient of 210 $Mbar^{-2}\mu s^{-1}$ using different equations of state. The value of G_1 for confined 170°C LX-04-01 listed in Table 2 is 130

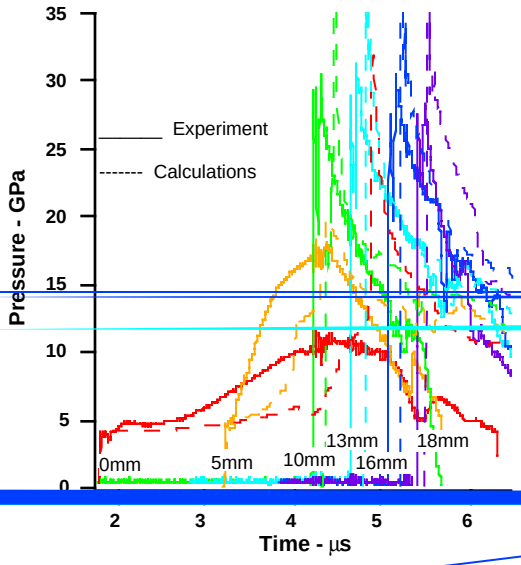

FIGURE 6. PRESSURE HISTORIES FOR UNCONFINED 25°C LX-04-01 IMPACTED BY TEFLON FLYER AT 1.279 KM/S

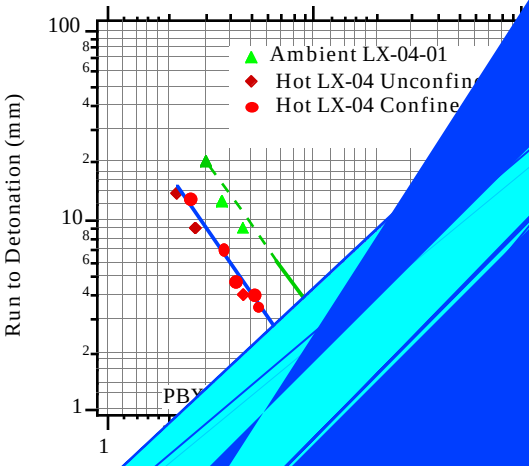

FIG

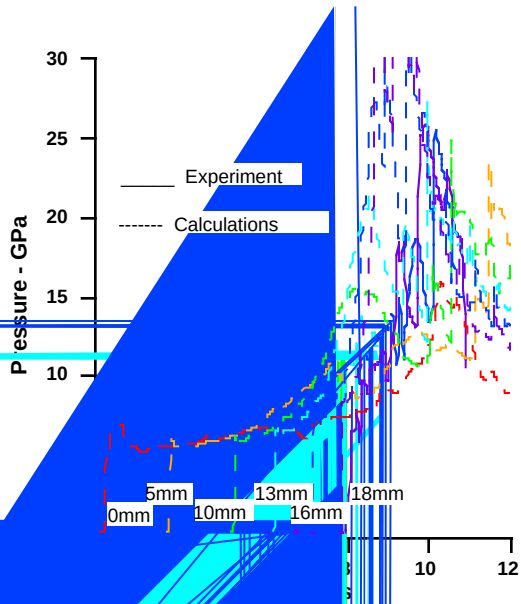

FIGURE 8. PRESSURE HISTORIES FOR STEEL CONFINED 250°C LX-17 IMPACTED BY A STEEL FLYER AT 0.988 KM/S

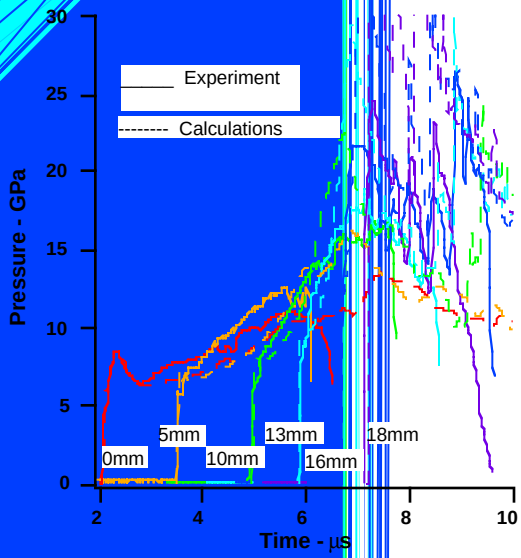

FIGURE 9. PRESSURE HISTORIES FOR STEEL CONFINED 250°C LX-17 IMPACTED BY A STEEL FLYER AT 1.11 KM/S

$Mbar^{-2}\mu s^{-1}$. Thus, there is a 30 percent difference in the growth of reaction coefficient G_1 required to calculate the experimental pressures in unconfined and confined 170°C LX-04-01.

The differences between heavily confined and

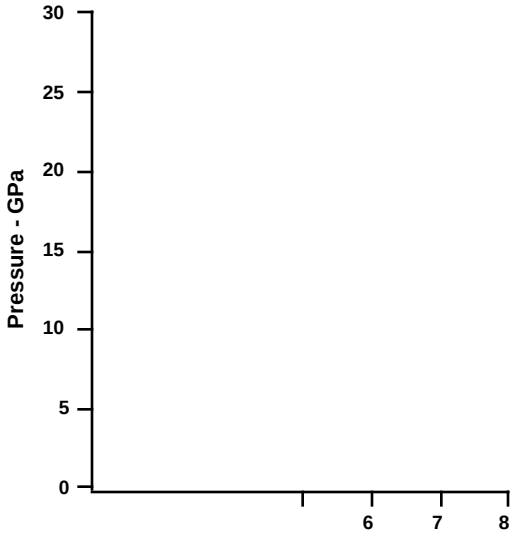

dependent on the relative strength of the material confining the explosive charge.

SUMMARY AND CONCLUSIONS

The steel confinement has a strong effect on inhibiting growth of the TATB crystals causing the sensitivity at 250°C to be considerably less than that measured under conditions of zero or weak confinement. The effect of steel confinement on the shock initiation of 170°C LX-04-01 is not as large as found for LX-17, because HMX crystals do not grow as much or as asymmetrically as do TATB crystals. Therefore, the shock sensitivity of LX-17 in scenarios in which it is heated to temperatures close to or even above its critical temperature and then subjected to fragment impact(s) depends strongly on the strength of its confining materials. Since the shock sensitivity of hot LX-04-01 was found to be far less dependent on its confinement, the high temperature shock sensitivity of LX-04-01 is similar in systems with very different containment strengths.

The Ignition and Growth reactive flow model parameters developed from embedded pressure gauge records taken under the various confinement and thermal conditions are frequently used to predict the possibility of shock initiation in hazard scenarios that can not be tested directly.

REFERENCES

1. Tarver, C. M., Hallquist, J. O., and Erickson, L. M., Eighth Symposium (International) on Detonation, Naval Surface Weapons Center NSWC 86-194, Albuquerque, NM, 1985, p. 951.

2. Urtiew, P. A., Erickson, L. M., Aldis, D. F., and Tarver, C. M., Ninth Symposium (International) on Detonation, Office of the Chief of Naval Research OCNR 113291-7, Portland, OR, 1989, p. 112.

3. Bahl, K., Bloom, G., Erickson, L., Lee, R., Tarver, C., Von Holle, W., and Weingart, R., Eighth Symposium (International) on Detonation, Naval Surface Weapons Center NSWC MP 86-194, Albuquerque, NM, 1985, p. 1045.

4. Urtiew, P. A., Cook, T. M., Maienschein, J. L., and Tarver, C. M., Tenth International Detonation Symposium, Office of Naval Research, ONR 33395-12, Boston, MA, 1993, p. 139.

5. Urtiew, P. A., Tarver, C. M., Maienschein, J. L., and Tao, W. C., Combustion and Flame 105, 43 (1996).

6. Tarver, C. M., Propellants, Explosives and Pyrotechnics 15,132 (1990).

7. Urtiew, P.A., Tarver, C. M., Forbes, J. W., and Garcia, F., Shock Compression of Condensed Matter-1997, S. C. Schmidt, D. P. Dandekar, J. W. Forbes, eds., AIP Conference Proceedings 429, Woodbury, NY, 1998, p. 727.

8. Dobratz, B. M., and Crawford, P. C., LLNL Explosives Handbook, UCRL-52997 Change 2, January 31, 1985.

9. Dallman, J. C. and Wackerle, J., Tenth International Detonation Symposium, Office of Naval Research, ONR 33395-12, Boston, MA, 1993, p. 130.

ACKNOWLEDGMENTS

The authors acknowledge technical discussions and support of this work by Jon Maienschein. Dan Greenwood designed and built the electrically shielded and isolated electronic cabinet housing the digitizers and power supplies. Paul Marples machined the parts for the experiments and helped assemble the electronics cabinet. Don Hansen, Barry Levine, Patrick McMaster, Gary Steinhour, and Ernie Urquidez assisted on the firing of the gun shots.

This work was performed under the auspices of the United States Department of Energy by the Lawrence Livermore National Laboratory under Contract No. W-7405-ENG-48.

TABLE 2. REACTIVE FLOW PARAMETERS FOR 250 $^{\bullet}$C LX-17 AND 170$^{\bullet}$C LX-04-01 CONFINED BY STEEL

A. 250 $^{\bullet}$C LX-17	ρ_0 =1.85 g/cm^3	
UNREACTED JWL	PRODUCT JWL	REACTION RATES
A=244.8 Mbar	A=13.454 Mbar	I=1.0x10^4 μs^{-1}
B=-0.045366 Mbar	B=0.6727 Mbar	a=0.20
R_1=11.3	R_1=6.2	b=0.667
R_2=1.13	R_2=2.2	x=7.0 F_{igmax}=0.02
ω=0.8938	ω=0.5	G_1=100 Mbar$^{-2}\mu$s^{-1}
C_V=2.487x10^{-5} Mbar/K	C_V=1.0x10^{-5} Mbar/K	c=0.667
T_0 = 523$^{\bullet}$K	E_0=0.067 Mbar	d=0.667
Shear Modulus=0.030 Mbar		y=2.0 F_{G1max}=0.5
Yield Strength=0.002 Mbar		G_2=400 Mbar$^{-3}\mu$s^{-1}
		e=0.333
		g=1.0
		z=3.0 F_{G2min}=0.5

B. 170 $^{\bullet}$C LX-04-01	ρ_0 =1.77 g/cm^3	
UNREACTED JWL	PRODUCT JWL	REACTION RATES
A=6046 Mbar	A=13.64355 Mbar	I=7.43x10^{11} μs^{-1}
B=-0.0633711 Mbar	B=0.718081 Mbar	a=0
R_1=14.1	R_1=5.9	b=0.667
R_2=1.41	R_2=2.1	x=20.0 F_{igmax}=0.3
ω=0.8867	ω=0.45	G_1=130 Mbar$^{-2}\mu$s^{-1}
C_V=2.7806x10^{-5} Mbar/K	C_V=1.0x10^{-5} Mbar/K	c=0.667
T_0 = 523$^{\bullet}$K	E_0=0.095 Mbar	d=0.333
Shear Modulus=0.0474Mbar		y=2.0 F_{G1max}=0.5
Yield Strength=0.002 Mbar		G_2=400 Mbar$^{-2}\mu$s^{-1}
		e=0.333
		g=1.0
		z=2.0 F_{G2min}=0.5

C. 25^{o}C Unconfined LX-04-01 ρ_0 =1.866 g/cm^3

T_0 = 298^{o}K B=-0.0487275 Mbar Shear Modulus = 0.05 Mbar G_1 = 90 Mbar$^{-2}\mu$s^{-1}

TABLE 3. GRUNEISEN EOS PARAMETERS FOR INERT MATERIALS

$$p=\rho_0 c^2\mu[1+(1-\gamma_0/2)\mu-a/2\mu^2]/[1-(S_1-1)\mu-S_2\mu^2/(\mu+1)-S_3\mu^3/(\mu+1)^2]^2 + (\gamma_0 + a\mu)E,$$

where $\mu = (\rho/\rho_0 - 1)$ and E is thermal energy

INERT	ρ_0(g/cm^3)	c(mm/μs)	S_1	S_2	S_3	γ_0	a
Al 6061	2.703	5.24	1.4	0.0	0.0	1.97	0.48
Steel	7.90	4.57	1.49	0.0	0.0	1.93	0.5
Teflon	2.15	1.68	1.123	3.98	-5.8	0.59	0.0